Fluorescent magnetic bead-based mast cell biosensor for electrochemical detection of allergens in foodstuffs

Donglei Jiang, Hui Jiang, Jian Ji, Xiulan Sun, He Qian, Genyi Zhang, Lili Tang

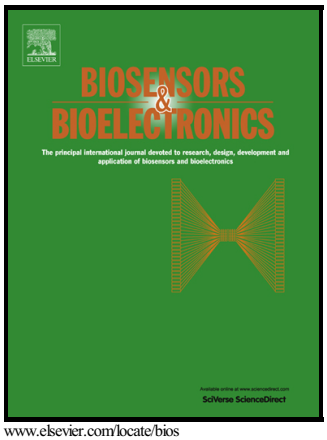

www.elsevier.com/locate/bios

PII: S0956-5663(15)00210-9
DOI: http://dx.doi.org/10.1016/j.bios.2015.03.058
Reference: BIOS7550

To appear in: *Biosensors and Bioelectronic*

Received date: 22 January 2015
Revised date: 17 March 2015
Accepted date: 23 March 2015

Cite this article as: Donglei Jiang, Hui Jiang, Jian Ji, Xiulan Sun, He Qian, Genyi Zhang and Lili Tang, Fluorescent magnetic bead-based mast cell biosensor for electrochemical detection of allergens in foodstuffs, *Biosensors and Bioelectronic,* http://dx.doi.org/10.1016/j.bios.2015.03.058

Fluorescent magnetic bead-based mast cell biosensor for electrochemical detection of allergens in foodstuffs

Donglei Jiang[a], Hui Jiang[a], Jian Ji[a], Xiulan Sun[a]*, He Qian[a], Genyi Zhang[a]*, Lili Tang[a]

[a]School of Food Science and Technology,State Key Laboratory of Food Science and Technology, Synergetic Innovation Center of Food Safety and Nutrition, Jiangnan University, Wuxi, Jiangsu 214122, China

***Author correspondence. Tel: +86 510-85329015, Fax: +86 510-85328726. E-mail: sxlzzz@jiangnan.edu.cn;**

ABSTRACT

In this study, a novel electrochemical rat basophilic leukemia cell (RBL-2H3) cell sensor, based on fluorescent magnetic beads, has been developed for the detection and evaluation of different allergens in foodstuffs.Fluorescein isothiocyanate (FITC) was successfully fused inside the SiO_2 layer of SiO_2 shell-coated Fe_3O_4 nanoparticles, which wassuperior to the traditional Fe_3O_4@SiO_2@FITC modification process. The as-synthesized fluorescent magnetic beads were then encapsulated with lipidosometo form cationic magnetic fluorescent nanoparticles (CMFNPs) for mast cell magnetofection. The CMFNPs were then characterized by SEM, TEM, VSM, FTIR, and XRD analyses, and transfected into RBL-2H3 cells through a highly efficient, lipid-mediated magnetofection procedure. Magnetic glassy carbon electrode (MGCE), whichpossesses excellent reproducibility and regeneration qualities, was then employed to adsorb the CMFNP-transfected RBL-2H3 cells activated by an allergen antigen for electrochemical assay. Results show that the exposure of model antigen-dinitrophenol-bovine serum albumin (DNP-BSA) to anti-DNP IgE-sensitized mast cells induced a robust and long-lasting electrochemical impedance signal in a dose-dependent manner.Thedetection limit was identified at3.3×10^{-4} ng/mL. To demonstrate the utility of this mast cell-based biosensor for detection of real allergens in foodstuffs, Anti-Pen a1 IgE and Anti-PV IgE-activated cells were employed to quantify both shrimp allergen tropomyosin (Pen a 1) and fish allergen parvalbumin (PV). Results show high detection accuracy for these targets, with a limit of 0.03

μg/mL (shrimp Pen a 1) and 0.16 ng/mL (fish PV), respectively. To this effect, we conclude the proposed method is a facile, highly sensitive, innovative electrochemical method for the evaluation of food allergens.

Key words: Fe_3O_4, FITC, SiO_2, lipidosome, RBL-2H3 mast cells, fish parvalbumin, shrimp tropomyosin Pen a 1, electrochemical impedance spectroscopy.

1. Introduction

Food allergies have become a serious public health concern, especially within the past few years. According to a recent survey, up to 4-5% of the total human population in industrialized countries suffers from a clinically-proven food allergy(Mehta et al., 2014). The prevalence of food allergies is estimated to be 10% in young children, and about 2-3% in adults (Muraro et al., 2014). Allergic reactions are momentarily disabling at best, and potentially fatal at worst (Niggemann and Beyer, 2014). The underlying causes and specific agents that lead to an allergic reaction are highly complex and heterogeneous (Abassi et al., 2004;Rockwood et al., 2013) . Exposure to food allergens induces an increase in the blood's immunoglobulin E (IgE) level, which triggers IgE-mediated type I allergies, such as allergic asthma, rhinitis, and atopic dermatitis (Bush, 2002; Sova et al., 2013; Yanase et al., 2012).Due to the fact that the introduction of even a very minimal concentration of an allergen can induce severe immunological reactions, successful and widely-available allergy management has become a crucial consideration for researchers and developers. A novel, effective method for detection of allergens in foodstuffs is a key component of allergy treatment, clearly, as it aids prevention of exposure to allergens.

There currently exist a number of technical approaches for identifying the presence of allergic proteins in food,includingmass spectrometry(Carrera et al.,2012),real-time polymerase chainreaction (RT-PCR)(Lopez and Pardo, 2010; Sun et al., 2009), and enzyme-linked immunosorbent assay (ELISA)(Fu and Maks, 2013; Zhang et al., 2014).Though these tests are highly specific and sensitive, their lengthy analysis time poses an obvious inconvenience to practical applications.Other possible methods for specific food allergen detection are based on the measurement of IgE-induced degranulation in vitro(Eccleston et al.,1973).For example, the rat basophilic leukemia (RBL-2H3) cell line possesses FcεR, which can selectively bind murine IgE antibodies so that subsequent encounters with an allergen will cross-link the FcεRI-IgE complex on the surface of mast cells(Curtis et al.,2008). This triggers a

sequence of intracellular events, including cellular degranulation and the release of chemical mediators such as histamine, serotonin, and β-hexosaminidase (Brockow, 2013; Corry and Kheradmand, 1999). Hence,RBL-2H3 mast cells show excellent potential for biosensor applications(Xin et al., 2014), due to their dramatic exocytotic response to antigen within minutes.They can detect target antigens and convert biological recognition into a signal that can be recorded and quantified quite easily(Kawakami and Galli,2002) .

As a noninvasive and sensitive detection technique for studying living cells, electrochemical impedance spectroscopy (EIS) measurementhas consistently proven valid, showing promising applicationto monitoradhesion, viability, and environmental changes in cells(Cortes-Salazar et al., 2013). Recent studies on biosensors have demonstrated that EIS measurements produce significantly more sensitive responses than cyclic voltammograms (CV)as far as fabrication of label-free cell-based biosensors(Asphahani and Zhang, 2007) . Thus, a sensitive and specific electrochemical signal generated by cells immobilized on an electrode can be detected rapidly and accurately, especially when exposed to an allergen.

Researchers and developers have grown increasingly interest in the application of nanomaterials to biosensors due totheirfavorable qualities such as large surface-to-volume ratio, high surface reaction activity, and strong adsorption ability(Malhotra et al., 2014;Yang et al., 2009).Fe_3O_4 nanoparticles, in particular, have become a favouritecandidate for biosensing, as they show distinct advantages of biocompatibility andenvironmental-safety(Shabani and Khodayari ,2015;Tang et al., 2003).To acquire stable and versatile fluorescent magnetic nanoparticles,adequate surface-coating materials are required. Silica is typically favored for encapsulating magnetic nanoparticles due to its stability, biocompatibility, simple functionalization, and low cytotoxicity(Zhang et al., 2010).Silica-coated fluorescent magnetic nanoparticleshave been recently investigated bymany researchers(Zhang et al., 2009).However, in these researches, these studies fabricated fluoresceinisothiocyanate (FITC) outside of the silicon oxide layer to form a fluorescent structure.Although this traditional Fe_3O_4@SiO_2@FITCmodified processis more convenient and feasible,its particularstructure does not benefit the combination of nanoparticles with positively-charged cationic liposomesorsatisfy the need of a desirable outer surfacefor further modifications.To address the above issues,a novel strategy of fusing the FITC inside the SiO_2 shellwas required.Such a core-shell structure wouldprevent fluorescence quenching of the nanoparticles,maintainphotochemical stability,provide

desirable negatively-changed surface and increase fluorescence intensityof the FITC dyes due to “caging effects” of silica shells.

Magnetofection is a novel, simple, and highly efficient method forcelltransfectionin culture(Krotz et al. 2003). It exploits the magnetic force to draw the vectors associated with magnetic particles toward or even into target cells.Using this method, the full vector dose applied is concentrated on the cells within a few minutes, so that 100% of the cells are in contact with a significant vector dose. At this point, liposomes can be combined with the fluorescent magnetic nanoparticles through electrostatic adsorption to formcationic magnetic fluorescent nanoparticles (CMFNPs).Thus, CMFNPs can replace vectors for cell uptake acceleration, promoting cell immobilization on the magnetic electrode.

This study explored a novel method for electrochemical determination of food allergens, based on cationic fluorescent magnetic bead-transferredRBL-2H3mast cells. The Fe_3O_4 nanoparticles were firstly synthesized and coated with silicon dioxide coupled with interior FITC. Fluorescent Fe_3O_4nanoparticles were then combined with liposomes for mast cell magnetofection. This is the first time that fluorescent magnetic beads were used as transfecting agents, taking advantage of magnetic fields for improving the efficiency of the system .The CMFNP-transferred living cells were then able to be rapidly isolated from the medium (with or without the targeted allergen) for electrochemical investigation.Different concentrations of DNP-BSA were employed as model samples to stimulate the anti-IgE DNP-sensitized RBL-2H3 cells for quantitative determination.Differing electrochemical responses caused by the stimulatory of shrimp and fish allergens on the mast cells are discussed below. Results of experimentation showed different dose-response correlations. The proposed method is ultimately proven simple, rapid, inexpensive, and convenient for electrode renewal, and is recommended as a promising experimental platform for wider applications in biosensing and cellular research.

2. Materials and methods

2.1. Materials and apparatus

Mouse monoclonal anti-dinitrophenyl IgE antibody (Clone SPE-7) and dinitrophenyl-bovine serum albumin (DNP-BSA), fluorescein isothiocyanate (FITC)and tetraethyl orthosilicate (TEOS) were obtained from Sigma-Aldrich Inc (St. Louis, MO, USA).Mouse monoclonal anti-shrimp tropomyosin IgEantibody was purchased from Santa Cruz Biotechnology (Dallas, TX, USA),Purified fish PVand mouse monoclonal anti-fish PV IgE antibody were purchased fromNovus Biologicals

(Littleton, CO), Purified shrimpPen a 1(tropomyosin)wasprepared by our lab (Jiang et al. 2013;).Iron chloride ($FeCl_3 \cdot 6H_2O$), sodium oleate, 3-aminopropyltriethoxysilane(APTES) and cyclohexane were from Shanghai Chemical Reagent Co (Shanghai, China). All other reagentswere of analytical grade and usedwithoutfurther purification. Rat basophilic leukemia (RBL-2H3) cells were obtained fromthe Cell Bank ofChinese Academy of Sciences (Shanghai, China). RPMI 1640 medium and fetal bovine serum were obtained fromGibco Invitrogen Corporation (CA, USA). All solutions were preparedwith deionized water and all reagents of analytical grade.

Allelectrochemicalexperiments were performed with anAuto Lab PGSTAT302N electrochemical workstation (Metrohm AutolabB.V., Utrecht, Netherlands). A homemade magneticglassy carbon electrode (MGCE) (Incole Union Technology Co, Ltd, Tianjin, China) was used as working electrode.A transmission electron microscope (TEM) (JEM-2100, Jeol,Japan), a scanning electron microscopy (SEM; model Hitachi S−4800, Hitachi Co., Ltd., Tokyo, Japan) and a Fourier transform infrared (FT-IR) spectrometer (FI-IR, NICOLET MEXUS 470, Thermo ElectronCorporation) were used to characterize the CMFNPs. RBL-2H3 cells were incubated in a CO_2incubator (Thermo Scientific Forma Series II Water Jacket,Thermo Fisher Scientific Inc., Rockford, IL, USA).A confocal laser scanning microscopy (LSM 710, Carl Zeiss Microscopy GmbH, Göttingen, Germany) was employed for the observationof magnetic fluorescent nanoparticles and cells.

2.2 *Preparation of fluorescent magnetic nanoparticles*

The magnetic nanoparticles (MNPs) were prepared according to a previouslyreported method(Wang et al. 2011). Briefly, 5.4 g of iron chloride (20 mM) and 18.5 gof sodium oleate (60 mM) were dissolved in a solvent mixture comprised of40 mLethanol, 30 mL distilled water and 70 mL hexane. The mixture solution was heatedto 70℃and stirred for 4 h. The upper organic layer was thenelutedby50 mL distilled water. Hexane was then evaporated off,led toan iron-oleate complex in a waxy solid form. 14 g of theiron-oleate complex (15.6 mM)and 2.0 g of oleic acid (7.0 mM) were dissolved in 20 g of1-octadecene at room temperature. The reaction mixture was heated to 320℃ata constant heating rate of 3.3℃min^{-1}, and continued to heat at that temperature for 1h.The reaction solution containing the nanocrystals was then cooled to roomtemperature, and 200 mL of ethanol was added to precipitate thenanocrystals. The nanocrystals were separated by centrifugation and then driedunder vacuum and stored at 4℃.

Fluorescein isothiocyanate (FITC) was firstcovalently linked to 3-aminopropyltriethoxysilane (APTES) by dissolving 10 mg of FITC in 48 mg of APTES (1:4 molar ratio).Cyclohexane was thenaddedto preparea 10vol% FITC/APTES in cyclohexane solution.This FITC/APTES/cyclohexane solution was stirred for 24 h in the dark before use.4mL of Igepal CO-520 were added to 80 mL of cyclohexane and stirred for 5 min. 2 mL of a cyclohexane dispersion ofFe_3O_4nanocrystals (5 mg/mL) were then added to the Igepal CO-520 and cyclohexane mixture and continued to stir for 5 min. 750mL of the FITC/APTES/cyclohexane solution were added dropwise to the nanocrystal dispersion, followedby the dropwise addition of 0.65 mL of 30%aqueous ammonium hydroxide solution. Due to the hydrolysis rate of APTES is five times slower than that oftetraethyl orthosilicate (TEOS)(Wang and Tan, 2006), the reaction was stirred for 24 h prior to theTEOS addition to ensure that the APTES bound to the FITC was hydrolyzed and FITC wouldbe incorporated in the SiO_2shell. Then 0.30 mL of TEOS was added dropwise to thesolution and the mixture was stirred for 48 h.

2.3. Cells culture and Magnetofection

RBL-2H3cells were cultured in a flask in RPMI 1640 mediumsupplemented with 10% fetal calf serum, penicillin (100 μgmL^{-1}),and streptomycin (100 μgmL^{-1})at37℃ in a humidified atmosphere containing 5% CO_2. At the growth retardation stage after3 d, cells reached to the logarithmic phase of growth after whichthey were used for experiments.

One day before magnetofection, plates were prepared containing 2×10^5RBL-2H3 cells in 500 µL of growth medium without antibiotics such that the cells were 90–95% confluent at the time of magnetofection.The process was carried outaccording to the manufacturer's instructions. Briefly, 100µL MFNPs (50mg/mL) were diluted in 100µL Opti-MEM® I Reduced Serum Medium without serum (Gibco® Invitrogen, Life Technologies) and mixed gently. 20µL of Lipidosome®2000 (Invitrogen, Life Technologies, Grand Island, NY, USA) were mixed gently before use, and added dropwise to100 µl of Opti-MEM® I Medium. After 5 minutes incubation at room temperature, diluted MFNPs were combined with the diluted Lipidosome® 2000and incubated for 20 minutes at room temperature.Then,the mixture was added dropwise to RBL-2H3 cell platesand mixed gently, washed with sterile phosphate buffered saline (PBS)after the cells immobilized completely under a magnetic field.

2.4 Assay ofCMFNPSCytotoxicityfor cell labeling.

Cytotoxicity of the prepared CMFNPs was evaluated bymethyl thiazolyl

tetrazolium(MTT)colorimetric assay. Cellswere seeded in a 96-well plate at a density of 5×10^3cells/well and incubated. After washing twice withfresh culture medium, cells were treated with the CMFNPs at concentrations from 2 to 50mg/mL for 24 h at 37 °C. Then, cells were washed twice withculture medium, and MTT solution (5 mg/mL in PBS) wasadded to each well and the cells were incubated at 37 °C.After 4 h, the media were removed and DMSO was added todissolve the formazan crystals. Ultraviolet absorbance at 570nm was measured with a microplate reader (BioTek Instruments, Inc., Winooski, VT, USA).The influence of CMFNPsmagnetofection on cellsurvival was examined by evaluating apoptosis via fluorescence-activated cellsorting analysis including an Annexin-V-EGFP Apoptosis DetectionKit (Nanjing KeyGen Biotech Co., Ltd., Shanghai, China). Briefly, RBL-2H3cells on 12-well plates wereharvested by trypsinization 3 d after infection with CMFNPs.Following neutralization by washing with culture media containing fetal bovine serum (FBS)and PBS, the cells were resuspended in 100 μL of annexin-V binding bufferand stained in the dark with 4 μL annexin-V/EGFP (an apoptosis marker) and 4 μL propidium iodide (PI, a necrosis marker) or 15 min at room temperature as a control. After adding400 μL of annexin-V binding buffer, 10,000 cells per sample wereanalyzed by flow cytometry and CellQuestsoftware. Fluorescent signals from EGFP and PI were distinguished by 3 color detectors.

2.5 RBL-2H3 sensor assay

A 1.5 mL tube wasprepared containing 200μL of CMFNPs transferredRBL-2H3 cell (1.6×10^9cells mL^{-1}) suspensionincubated with three to five-fold molar excess of anti-DNPIgE antibody (or anti-Pen a 1 IgE and anti-PV IgE) for 30min incubation at 37 ℃.Next 50 μL of seriallydiluted DNP-BSA antigen (or purified shrimp tropomyosin antigen and purified fish PV antigen) were addedtothe tube and mixed with cells by pipetting for 1 min,then incubated at 37 ℃for 5 min. The reactionwas stopped by placing the tube at 4 ℃ for1 min.Then, in order to remove theCMFNPsexpelledfrom the RBL-2H3 cellsundercelldegranulation,cell suspension was then filtered by theTc-s0037Cell Strainer(1200 mesh, 11μm,Toscience Biotechnology Co., Ltd.shanghai, China)coupled with 50mL centrifuge tube, and centrifugedat 1000rpm for 5 min.Due to the different sizes of cells and CMFNPs (mast cell size=30μm, CMFNPs size=200nm), they could be well separated through the Cell Strainer and centrifugal force.The harvestedRBL-2H3cells were then washed and maintained in Tyrode's buffer in 2mL tube. After that, a magnetic glassy carbon electrode (MGCE)wasinsertedinto the bottom of the tube to gather the RBL-2H3 cells

for electrochemical analysis.(It was important to always keepthe glassy carbon sideof magnetic electrode in headstandposition during the measurementto prevent the immobilization of RBL-2H3 cells on the electrode undergravity.) All the electrochemical experiments were performed using anAutoLab electrochemical workstation (Auto Lab PGSTAT302N, USA). The supporting electrolyte used was a 1 × PBS containing a 1 mM $Fe(CN)_6^{3-}$/$Fe(CN)_6^{4-}$(1:1) redox pair. Differential pulse voltammetry (DPV), cyclic voltammetry (CV)and impedance measurements were carried out in a conventionalthree-electrode cell. An Ag/AgCl electrode and Pt wire were usedas the reference and counter electrode, respectively. The potentialscan range for the CV and DPV was −0.2 to +0.6 V with a scan rate of 50 mV/s.For the impedance measurement, a DC bias voltage was set at theopen-circuit potential of the redox pair with a 5 mV AC amplitude ina test frequency ranging from 1 Hz to 100 kHz. Cells not exposed to DNP-BSA (purifiedshrimp tropomyosin antigen and fish PV antigen) served as the control.

3. Results and discussion

3.1. Working principles of RBL-2H3 cell sensors.

Scheme 1 illustrates the preparation of the CMFNP -transferred RBL-2H3 cell sensor and the working principle of theRBL-2H3 cell sensor for recognizing and quantifyingthe target allergen.Fluorescein isothiocyanate (FITC) was successfully fused inside the SiO_2 layer of SiO_2 shell-coated Fe_3O_4nanoparticles. The as-synthesized fluorescent magnetic beads were then encapsulated with liposome to form cationic magnetic fluorescent nanoparticles (CMFNPs) and were transfected into RBL-2H3 cells through the magnetic Field. When the CMFNP -transferred RBL-2H3 cells attached to the magnetic electrode's surface, they created a barrier against the electrochemical process, hindering the redox probe from accessing the electrode surface and resulting in increased electron-transfer resistance(Haoet al., 2007). However, if an allergen antigen, such as DNP-BSA, was employed to stimulate the DNP-IgE pre-sensitized mast cell, it would trigger CMFNP -transferred RBL-2H3 cell degranulation and release of inflammatory mediators which wouldlead to cell apoptosis and cell death. A portion of CMFNPs wouldthen be expelled from the cells, causing decrease in cell magnetism and prevention of absorption by the magnetic electrode, where the electron transfer rate of the working electrode was accelerated, resulting in decrease in electron-transfer resistance (Jiang et al., 2013). Thus, a sensitive and specific electrochemical signal generated by CMFNP -transferred RBL-2H3 cell absorbed on the magnetic electrode can be detected rapidly and

accurately, especially when exposed to an allergen.

3.2. Synthesis and characterization of magnetic fluorescent nanoparticles

A typical Fe_3O_4 dispersion uses magnetic cores, which are synthesized by thermal decomposition of an iron-oleate. In order to maintain the surface positive charge of the fluorescent magnetic nanoparticles, FITC covalently linked to APTES wasfirst used to disperse the nanocrystals through electrostatic adsorption. FITC–APTES conjugates were prepared in advance via an addition reaction between the iso-thiocyanate group of FITC dye and the APTES's primary amine group. Next, TEOS was employed to form a SiO_2 shell that completely encapsulated the FITC-transferred Fe_3O_4 nanoparticle interiors. Since the hydrolysis rate of APTES is five times slower than that of tetraethyl orthosilicate (TEOS), the reaction was stirred for 24h prior to TEOS addition to ensure that the APTES as-bound to the FITC was hydrolyzed effectively for incorporation into the SiO_2 shell (Wang et al., 2011). The synthetic process thus effectively enabled the co-encapsulation of Fe_3O_4 nanoparticles plus a large amount of FITC dye molecules inside the silica shell, while maintaining theelectronegativity of the silica surface.

Transmission electron microscopy (TEM) images of Fe_3O_4 nanoparticles and magnetic fluorescent nanoparticles are shown inFig.1A and B.Fe_3O_4 nanoparticles prepared via the high-temperature thermal decomposition method were monodispersed with an average diameter of 160nm (Fig.1A).A thick layer of silica shell was then formed in situ through hydrolysis of tetraethyl orthosilicate (TEOS) and subsequent condensation of silica onto the surface of Fe_3O_4 cores, measured at 16nm.The thickness of the silica shell can be adjusted by varying the volume of TEOS used. A TEM image of fluorescent magnetic nanoparticles shows well-defined, spherical core-shell structures with an average size of 185nm (Fig.1B).TheSEM image of the Fe_3O_4 nanoparticles and magnetic fluorescent nanoparticles also indicates that thesenanoparticles were uniform, round, and evenly distributed, even when dried (Figs. 1C and D).Additional information on the characteristics of Fe_3O_4 nanoparticles and magnetic fluorescent nanoparticles was provided in the supplementary material section(Fig.S1).

3.3RBL-2H3 mast cell transferred with CMFNPs by magentofection

Magentofection ofRBL-2H3 mast cells with CMFNPs mainly involves theelectrostatic adsorption of magnetic fluorescent nanoparticles with lipidosome, and the incubation of CMFNPs with cells. To verify theCMFNPs as successfully transferredinto RBL-2H3 cells,an LSM 710 CLS microscope was employed to detect

fluorescent magnetic nanoparticle uptake in the RBL-2H3 cells after the cells were incubated with theCMFNPs. As shown in Figs. 2A and B, the presence of CMFNPs within the RBL-2H3 cells is quite clear. Almost 90% of cells show the bright green fluorescence characteristic of successful magnetofection.

Samples were kept on ice and further analyzed by flow cytometer at a minimum of 1×10^5cells. Uptake efficiency was calculated as the ratio of the number of fluorescence-transferred cells (CMFNP-endocytosed cells) to the initial cultured cells.Uptake efficiency was more than 85%, regardless of lipidosome encapsulation.For the CMFNPs, uptake efficiency reached about 91%, shown in Fig. 2C.MTT tests investigated potential adverse effects of the magnetofection process, where results show that the CMFNPs -transferredRBL-2H3 cells exhibited the same viability as the un-transferredRBL-2H3 cells, asshown in Fig. 2D. There is no correlation between CMFNP concentration and cell viability; in all cases, viabilities were above 90% and not significantly different from the control ($P > 0.05$). Therefore, cell viability of the RBL-2H3 cells was not negatively influenced by CMFNP labeling. Furthermore, flow cytometric analyses at Day 3 for the CMFNP-transferred cells(Fig. 2F) and control groups (Fig. 2E), using annexin V-EGFP and PI as markers for apoptosis and necrosis, respectively, disclosed similarly low rates of early apoptosis (0.24± 0.16 vs. 0.17± 0.15%, respectively), and necrosis (0.74 ±0.13 vs. 0.63 ± 0.15%, respectively).

3.4 Electrochemical characteristics of magnetic RBL-2H3 mast cell sensor

The characteristics of the CMFNP -transferredRBL-2H3 cells on magnetic GE were also tested by cyclic voltammetry (CV), differential pulse voltammetry (DPV), and electrochemical impedance spectra (EIS) in the presence of 2.5 mM $Fe(CN)_6^{3-/4-}$(Zahradnik et al., 2011). As shown in Fig. 3A, the voltammograms showed a typical, reversible redox peak at the bare GCE surface (Curve a).The redox current decreased rapidly when the electrode was flooded with CMFNP-transferredRBL-2H3 cells (Curve d)due to cell adhesion, where the electron transfer rate of the working electrode was blocked.The redox peak current increased after DNP-BSA was employed to stimulate the mast cell (Curve c), which led to cell allergic reaction and cell apoptosis as well as cell magnetism decrease. The number of cells absorbed by the magnetic electrodehaddeclined which causedelectron-transfer resistance to decrease.The redox current slightly decreased when the electrode was treated with CMFNPs lacking RBL-2H3 cells (Curve b), owing toa blocking effect caused by the electrical insulator properties of silicon dioxide encapsulated around the Fe_3O_4 core.

The electrochemical sensing ability of the cells was measured based on the observation that living cells are highly insulating at low frequencies. When CFMNPs-transferred cells adhered to the modified electrode, increased charge-transfer impedance was observed. This increase represents the combined effects of the reduction in the DPV current peak value (Fig. 3B) and the increase in EIS impedance value (Fig. 3C).As shown in Fig. 3B, DPV current peak value changes, found with CMFNP -transferred cells absorbed on the electrode, also showed increased coverage rate of MGCE, which impeded the current circulation (Curve d). When exposed to DNP-BSA, the peak current dramatically increased (Curve c) but was still lower than the sample withsolely CMFNPs attached to the magnetic electrode (Curve b).Fig. 3D shows that any increase in impedance was dependent on the surface's cell coverage, which was proportional to the concentration of the cells in a certain range.The R_{et} showed a linear relationship with cell concentration from 1.6×10^{3} to 1.6×10^{9}cells mL^{-1},with a correlation coefficient of 0.996. In addition, when cell numbers were more than 1.6×10^{9}, the impedance values were practically unchanged. The detection limit was calculated at about 640cells mL^{-1}, (based on the typical definition as three times the standard deviation of a blank sample.)Therefore, the appropriate cell number of 1.6×10^{9}cells $mL^{-1}$was selected for allergen analysis according to the results of R_{et} measurement.

3.5RBL-2H3 cell sensor assays for allergen detection

In this study, DNP-BSA was applied to indicate the R_{et} variation tendency of IgE-mediated hypersensitivity.Fig. 4 shows typical electrochemical impedance signals from RBL-2H3 cells activated by different concentrations of DNP-BSA. The R_{et} decreased as DNP-BSA concentration increased, where the diameter of the semi-circle on the Nyquist diagram shrinks (Fig. 4A). This implies a lower number of cells were absorbed on the magnetic electrode. Lower concentration of DNP-BSA stimulates cell degranulation, allowing the R_{et}toincrease due to the release of cytoplasm to the intercellular spaces of various chemicals such as histamine, tryptase, and β-hexosaminidase. RBL-2H3 cells still maintain a certain level of magnetism dependent on the remaining CMFNPs within the cells that were able tobe absorbed by the magnetic electrode.Higher DNP-BSA concentration inducedcell apoptosis and cytolysis(Rohlich et al. 1971), which causedcell lysis and excludes CMFNPs from the cell cytoplasm, causing both a decrease in cell magnetism and decline in R_{et} values.

Fig.4B shows the calibration curve for DNP-BSA obtained through experimentation in this study.The *y*-axis shows R_{et} estimated using information from

Fig. 4A.We measured precise DNP-BSA concentration ranging from 1×10^{-3} to 10^{4} ng/mL with very small error bars over a duration of less than 10 min. The detection limit was calculated at 3.3×10^{-4} ng/mL according to the formula LOD=3*s*/*m*, where *s* represents the standard deviation of the blank sample (n =3) and *m* represents the slope of the relative calibration curve for DNP-BSA.Results indicated that the quantitative performance for allergen modeling was superior to previous electrochemical assay (Jiang et al., 2013).Calibration curves for shrimp allergen Pen a 1 (tropomyosin) and fish allergen parvalbumin (PV) were also obtained using this test method. We measured precise fishPV and shrimp Pen a1 concentrations ranging from 0.5 to 4.5 ng/mL and 0.1 to 1.5μg/mL, respectively.The limits of detection (LOD) werecalculated at 0.16 ng/mL and 0.03μg/mL according to the formula LOD=3*s/m* (Figs. 4C and D).The obtained results were compared with other reported methods(Table S1).Most of these methods required complicated sample pretreatment procedures and were susceptible to contamination as well as high false-positive rates.The detection limits obtained by thisRBL-2H3cell sensors were lower, however, and the detection times were shorter than most of these methods, which provesthat the proposedbiosensor can meet thesensitivity requirements of applications for foodallergen investigation.

3.6Real sample measurements

To assess the RBL-2H3 sensor's ability to rapidly detect target allergens from real food samples, crucian carp and brown shrimp crude extra were used to test the performance of the proposedsensor. As shown inthe supplementary material (Fig.S3), purified Pen a 1 and PV wereapplied to the gel and SDS-PAGE was performed. Two major protein band werepresent at 36 kD and 12 kD,which were identified by Coomassie blue staining (Fig.S3A and B, with arrows).This demonstrated substantial purification on Pen a 1and PV.The activation of cell sensors with these two extracts also led to a rapid and robust decrease in cell impedance. The concentrations and contents of Pen a 1 and PV in samples, calculated from the standard curve of impedance versus PV and Pen a 1 standards according to Fig. 4 C and D, are shown in Table 1.The results obtained using the RBL-2H3cell sensors were similar to previouslyreported methods, which confirmsthat the proposedbiosensor can be applied effectively for detection and prediction ofreal allergen samples.

3.7 Specificity and reproducibility of the RBL-2H3 cell sensor

The specificity of the cell sensor plays an important role in analyzing biological samples in situ without separation. RBL-2H3 sensors pre-sensitized with anti-fish PV

were introduced to different allergens in turn, including shrimp allergen Pen a 1,soybean allergen *β*-conglycinin, and peanut allergen Ara h 1 (all prepared by our laboratory.)Non-specific interactions between cells and antigens were excluded by challenging un-sensitized RBL-2H3 sensor cells alongside pre-sensitized cells. Results show that non-corresponding allergen proteins hardly produced any response in R_{et} value. Anti-fish PV-pre-sensitized RBL-2H3 cells did not recognize the shrimp allergen, soybean allergen or peanut allergen.We thus posit that the RBL-2H3 cell sensor displays favorable specificity for the determination of food allergen proteins.

For magnetic electrode regeneration, after testing, the MGCE surface was rubbed with an alcohol pledget and washed with purified water to regenerate the magnetic electrode. Next, the MGCE was cleaned in 0.5mol/L H_2SO_4 by performing CVs from −1.0 to 1.0 V (vs. SCE) with a scan rate of 100mV/s for 20 cycles. After thoroughrinsing with purified water and dryingwith high-purity nitrogen gas (99.999%), the MGCE was used to capture mast cells with CMFNPs for all subsequent detection experiments.Ten spiked samples at two different concentrations,1,000 and 10,000 cells/mL, were tested by the cell sensor. Results are shown in Table S2.The recovery values were determined by testing cell samples at different concentrations. As shown in Supplement Table S1, the results show successful average recovery rates from 97.77% to 99.55% and coefficients of variance (CV) from 2.32% to 7.71%. These values are in accordance with the required accuracy in typical trace analysis, indicating easy reproducibility of the fabrication protocol.

4. Conclusion

In this study, a highly sensitive, facile, and successful magnetic fluorescent mast cell-based sensor was developed by absorbing living mast cells transferred with CMFNPs on MGCE, in effort to accurately quantify food allergens.Cationic magnetic fluorescent nanoparticles were synthesized, characterized,andtransferred into RBL-2H3 cells using magnetofection.The sensor exhibited favorable correlation with the logarithmic value of cell numbers, ranging from 1.6×10^{3} to 1.6×10^{10} cells·mL^{-1}. Exposure to DNP-BSA, a model allergen antigen, induced a robust and dose-dependent impedance signal. This confirms the following: 1) impedance changes indicated the presence of target antigens, and 2) RBL-2H3 cell sensor responses can be monitored in real-time by electrochemistry. R_{et} values were proportional to model DNP-BSA concentrations, ranging from 1×10^{-3} to 10 ng·mL^{-1}, with a correlation coefficient of 0.996 at a detection limit of 3.3×10^{-4} ng/mL (R.S.D. 5%). The detection

signal intensity of R_{et} was reduced as DNP-BSA concentrations decreased, corresponding to an increased semi-circle diameter in the Nyquist diagram. Theproposedmethod was successfully applied to quantify fish PV concentrations from 0.5 to 10 ng/mLwith a detection limit of 0.16 ng/mL (R.S.D. 4.5%),and shrimp allergen Pen a 1 concentrations from 0.1 to 6 μg/mL, with a detection limit at 0.03μg /mL (R.S.D. 4.6%). The proposed cell sensor is simple, rapid, inexpensive, and convenient for electrode renewal. The method is recommended for wider application in biosensing and cellular research, based on known information for many other cells/magnetic nanomaterials.

Acknowledgements

This work has been supported by National research program(No. 2011BAK10B03) , "973" National Basic Research Program of China (No. 2012CB720804), Program for New Century Excellent Talents in Jiangnan University , Commonweal project of the Ministry of Agriculture (No. 201203069－1), and, and the Priority Academic Program Development of Jiangsu Higher Education Institutions.

Reference

Abassi, Y.A., Jackson, J.A., Zhu, J., O'Connell, J., Wang, X.B., Xu, X., 2004. Journal of Immunological Methods 292(1-2), 195-205.

Asphahani, F., Zhang, M., 2007. Analyst 132(9), 835-841.

Brockow, K., 2013. Mast cell activation syndrome. Hautarzt 64(2), 102-106.

Bush, R.K., 2002. Medical Clinics of North America 86(5), 1113.

Carrera, M., Canas, B., Gallardo, J.M., 2012. Journal of proteomics 75(11), 3211-3220.

Corry, D.B., Kheradmand, F., 1999. Nature 402(6760), B18-B23.

Cortes-Salazar, F., Beggah, S., van der Meer, J.R., Girault, H.H., 2013. Biosensors and Bioelectronics 47, 237-242.

Curtis, T., Naal, R.M.Z.G., Batt, C., Tabb, J., Holowka, D., 2008. Biosensors and Bioelectronics 23(7), 1024-1031.

Eccleston, E., Leonard, B.J., Lowe, J.S., Welford, H.J., 1973. Nature: New biology 244(133), 73-76.

El-Boubbou, K., Gruden, C., Huang, X., 2007. Journal of the American Chemical Society 129(44), 13392.

Fu, T.-J., Maks, N., 2013. Journal of Agricultural and Food Chemistry 61(24), 5649-5658.

Hao, C., Yan, F., Ding, L., Xue, Y., Ju, H., 2007. Electrochemistry Communications 9(6), 1359-1364.

Jiang, D., Ji, J., An, L., Sun, X., Zhang, Y., Zhang, G., Tang, L., 2013. Biosensors and Bioelectronics 50, 150-156.

Jiang, D., Jiang, H., Ji, J., Sun, X., Qian, H., Zhang, G., Tang, L., 2014. Journal of Agricultural and Food Chemistry 62(27), 6473-6480.

Kawakami, T., Galli, S.J., 2002. Nature Reviews Immunology 2(10), 773-786.

Krotz, F., de Wit, C., Sohn, H.Y., Zahler, S., Gloe, T., Pohl, U., Plank, C., 2003. Molecular Therapy 7(5), 700-710.

Lopez, I., Angel Pardo, M., 2010. Journal of Agricultural and Food Chemistry 58(3), 1469-1477.

Malhotra, B.D., Srivastava, S., Ali, M.A., Singh, C., 2014. Applied Biochemistry and Biotechnology 174(3), 880-896.

Mehta, H., Ramesh, M., Feuille, E., Groetch, M., Wang, J., 2014. Journal of Pediatrics 165(4), 842-848.

Muraro, A., Hoffmann-Sommergruber, K., Holzhauser, T., Poulsen, L.K., Gowland, M.H., Akdis, C.A., Mills, E.N.C., Papadopoulos, N., Roberts, G., Schnadt, S., van Ree, R., Sheikh, A., Vieths, S., Allergy, E.F., Anaphylaxis Guidelines, G., 2014. Allergy 69(11), 1464-1472.

Niggemann, B., Beyer, K., 2014. Allergy 69(12), 1582-1587.

Rockwood, J., Morgan, M.S., Arlian, L.G., 2013. Experimental and Applied Acarology 61(3), 311-325.

Rohlich, P., Anderson, P., Uvnas, B., 1971. The Journal of cell biology 51(21), 465-483.

Shabani, F., Khodayari, A., 2015. Synthesis and Reactivity in Inorganic Metal-Organic and Nano-Metal Chemistry 45(3), 356-362.

Sova, C., Feuling, M.B., Baumler, M., Gleason, L., Tam, J.S., Zafra, H., Goday, P.S., 2013. Nutrition in Clinical Practice 28(6), 669-675.

Sun, M., Liang, C., Gao, H., Lin, C., Deng, M., 2009.. Journal of Aoac International 92(1), 234-240.

Tang, J., Myers, M., Bosnick, K.A., Brus, L.E., 2003. Journal of Physical Chemistry B 107(30), 7501-7506.

Wang, L., Neoh, K.G., Kang, E.-T., Shuter, B., 2011. Biomaterials 32(8), 2166-2173.

Wang, L., Tan, W.H., 2006. Nano Letters 6(1), 84-88.

Xin, W., Yao, W., Gao, X., You, Z., Gao, S., Kang, L., Li, Q., Zhou, Y., Yang, H., Jiang, P., Wang, J., 2014. Journal of Biomedical Nanotechnology 10(11), 3318-3328.

Yanase, Y., Hiragun, T., Yanase, T., Kawaguchi, T., Ishii, K., Hide, M., 2012. Biosensors and Bioelectronics 32(1), 62-68.

Yang, H., Chen, S., Li, C., Chen, D., Ge, Z., 2009. Progress in Chemistry 21(1), 210-216.

Zahradnik, E., Sander, I., Bruckmaier, L., Flagge, A., Fleischer, C., Schierl, R., Nowak, D., Sueltz, J., Spickenheuer, A., Noss, I., Bruening, T., Raulf-Heimsoth, M., 2011. International Archives of Allergy and Immunology 155(3), 225-233.

Zhang, G., Feng, J., Lu, L., Zhang, B., Cao, L., 2010. Journal of Colloid and Interface Science 351(1), 128-133.

Zhang, H., Lu, Y., Ushio, H., Shiomi, K., 2014. Food Chemistry 150, 151-157.

Zhang, Y., Gong, S.W.Y., Jin, L., Li, S.M., Chen, Z.P., Ma, M., Gu, N., 2009. Chinese Chemical Letters 20(8), 969-972.

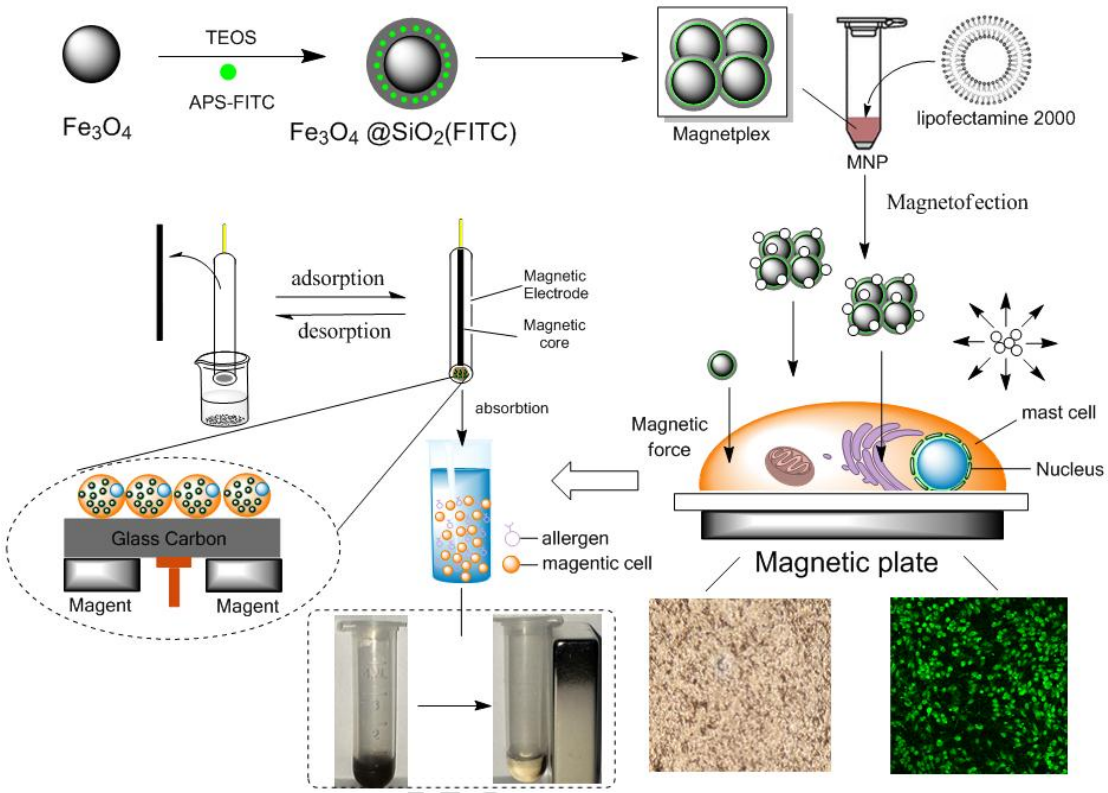

Scheme1. Schematic illustration of the preparation of magnetic RBL-2H3 cell sensor and process of allergen detection.

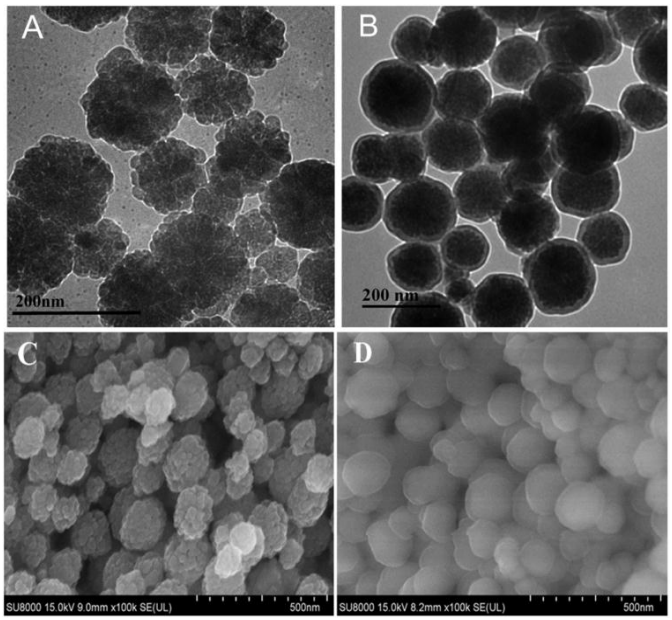

Figure1.TEM and SEM micrograph of (A, C) Fe_3O_4nanoparticles and (B, D) magnetic fluorescent nanoparticles

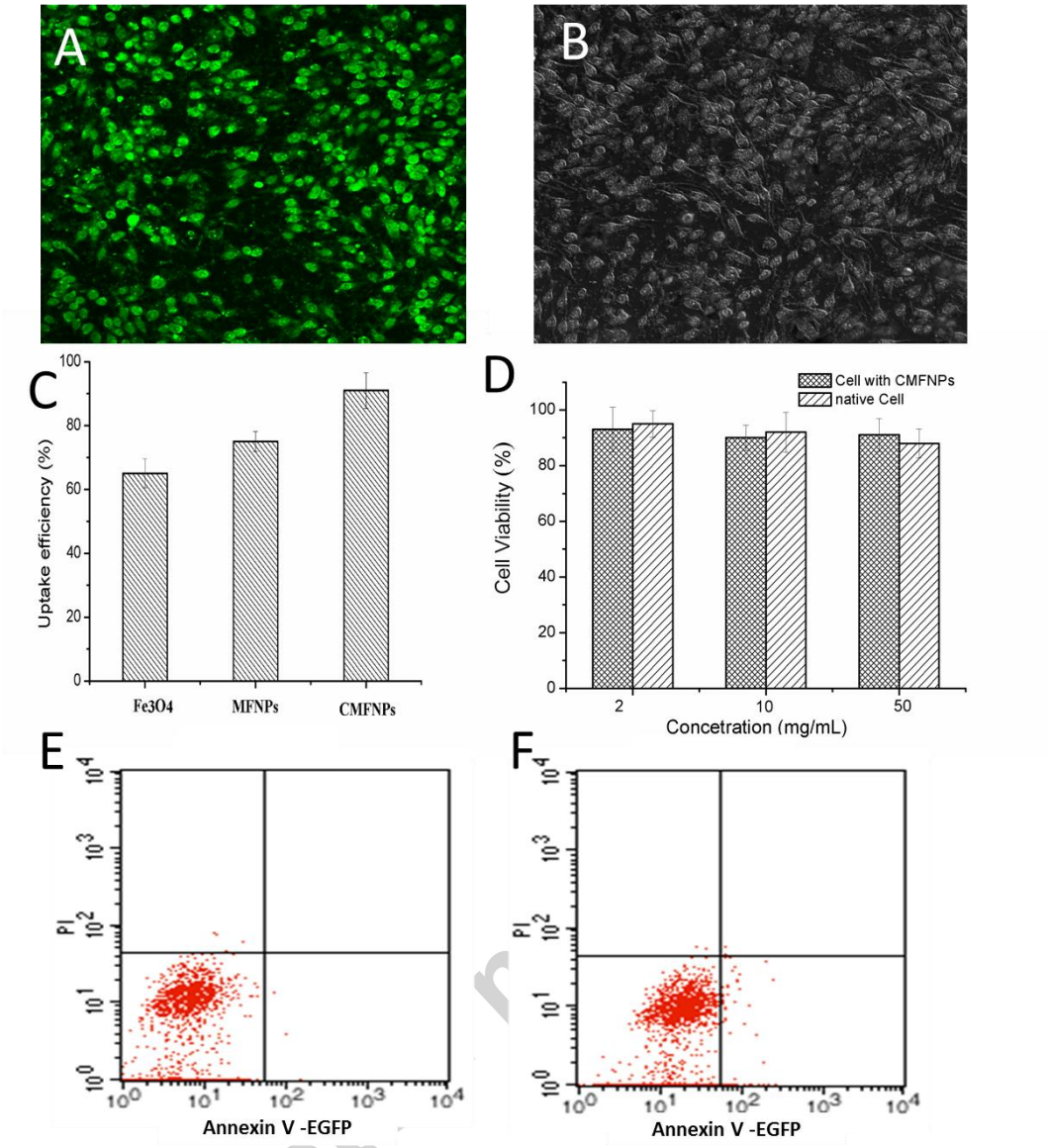

Figure2. Efficiency of CMFNPs magnetofection and influence on cell proliferation and survival. (A) Fluorescent detection of CMFNPs in RBL-2H3 cells by magnetofection (B) Morphology and density of CMFNPs transferred RBL-2H3 in bright field flow analysis. (C) Cellular uptake efficiency byRBL-2H3 cells treated with three different nanoparticles by flow cytometry. (D) Viability of RBL-2H3cells incubated with CMFNPs at different concentrations for 24 h. Control experiments were carried out without CMFNPs. FACS analysis of apoptosis in control (E) and CMFNPs transferred RBL-2H3 cells (F). The lower left quadrant contains annexin V-EGFP (-) and PI (-) viable cells; the lower right quadrant, annexin V-EGFP (+) and PI (-) early apoptotic cells; the upper right quadrant, annexin V-EGFP (+) and PI (+) late apoptotic or necrotic cells; the upper left quadrant, annexin V-EGFP (-) and PI (+) necrotic cells. Bars indicate % of apoptotic or necrotic cells in each group expressed as mean ± SD of data obtained from three independent experiments.

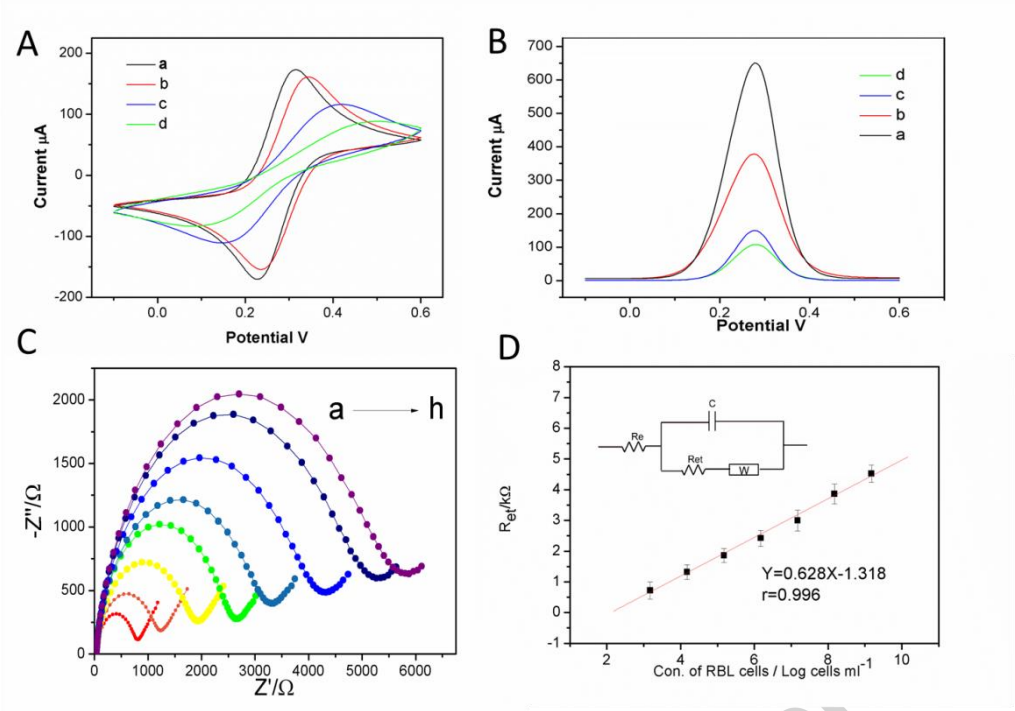

Figure 3.(A) Cyclic voltammograms of (a) bare MGCE,(b) MGCE with CMFNPs,(c)CMFNPs transferredRBL-2H3 cells treated with 100ngmL^{-1} DNP-BSA on MGCE,(d)MGCE with CMFNPs transferredRBL-2H3 cells.(B)Differential pulse voltammetry (DPV) of (a) bare MGCE,(b) MGCE with CMFNPs,(c) CMFNPs transferredRBL-2H3 cells treated with 100 ngmL^{-1} DNP-BSA on MGCE,(d) MGCE with CMFNPs transferredRBL-2H3 cells.(C) Nyquist diagrams of (a) 1.6×10^{3} cells mL^{-1}, (b) 1.6×10^{4} cellsmL^{-1}, (c) 1.6×10^{5} cells mL^{-1},(d) 1.6×10^{6} cells mL^{-1}, (e) 1.6×10^{7} cells mL^{-1}, (f) 1.6×10^{8} cellsmL^{-1},(g) 1.6×10^{9} cellsmL^{-1},(h) 1.6×10^{10} cellsmL^{-1}RBL-2H3 cells immobilized on electrode. (D) Equivalent circuit model, to which all of the experimental impedance curves were fitted.

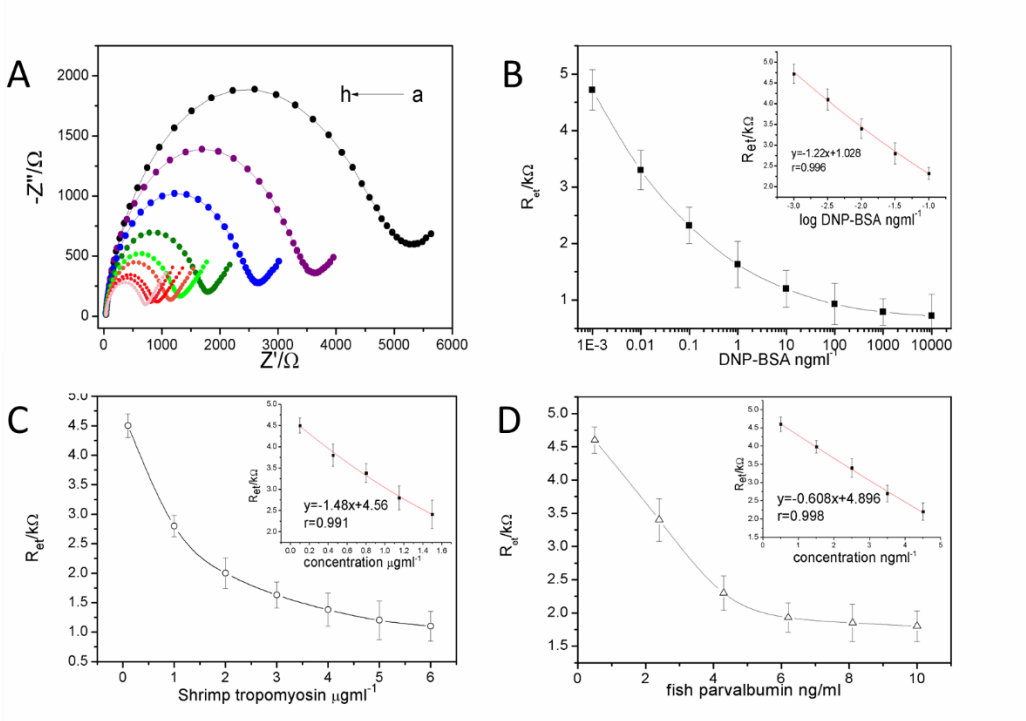

Figure 4. (A)Nyquist diagrams ofelectrochemical impedance spectroscopy for RBL-2H3 cells treated with different doses of DNP-BSA.(a→h)arrow indicates:1×10^{-3}ng·mL^{-1}, 1×10^{-2}ng·mL^{-1}, 1×10^{-1}ng·mL^{-1}, 1ng·mL^{-1}, 10ng·mL^{-1}, 100ng·mL^{-1}, 1×10^{3}ng·mL^{-1}, 1×10^{4}ng·mL^{-1}.(B) Calibration curveof DNP-BSA obtained with the proposed assay. The inset shows an expanded calibration curve in a low concentration range. (C)Quantification of major shrimp allergen by this cell sensors, inset: an expanded Calibration curve in a low concentration range. (D) Quantification of fish allergen parvalbumin allergen by this cell sensors, inset: an expanded Calibration curve in a low concentration range.

Table1. The concentration and content of parvalbumin and shrimp Pen a 1in real sample

Sample	Crucian carp	brown shrimp
Impedance value R_{et}（kΩ±SD）	0.98±0.08	2.18±0.15
concentration(ng/ml±SD)	4.31±0.22	1320±0.33
content (mg/g±SD)	2.12±0.23	39.5±0.26

SD, standard deviation (n = 5).

Highlights

- RBL-2H3 mast cell-based sensor for evaluating allergens in foodstuffs was developed.
- Fluorescent magnetic beads were prepared by fusing FITC inside the SiO_2 layer of SiO_2 shell-coated Fe_3O_4 nanoparticles and encapsulating them with lipidosome to form cationic magnetic fluorescent nanoparticles (CMFNPs) for mast cell magnetofection
- The fabricated CMFNPs show good biocompatibility and non-toxicity, and are used to efficiently label the RBL-2H3 cells.
- Electrochemical signal of cell showed an excellent linear relationship with the DNP-BSA, shrimp allergen Pen a 1and fish allergen parvalbumin, providing potential applications in allergen detection
- Magnetic electrode showed excellent regeneration and successful average recovery rates